Scanning Microscopy

Volume 1992
Number 6 *Signal and Image Processing in Microscopy and Microanalysis*

Article 14

1992

Some Applications of Image Analysis to Materials Science

François Grillon
Centre des Matériaux P.M. Fourt, France

Scanning Microscopy Supplement 6, 1992 (pages 147-151) 0892-953X/92$5.00+.00
Scanning Microscopy International, Chicago (AMF O'Hare), IL 60666 USA

SOME APPLICATIONS OF IMAGE ANALYSIS TO MATERIALS SCIENCE

François Grillon

Department Microscopy Analysis Photography, Centre des Matériaux P.M. Fourt, CNRS UA866
B. P. 87, F-91003 Evry Cedex, France
Telephone number: (33)-1-6076 3034 / FAX number: (33)-1-6088 4757

Abstract

We have presented four applications of Image Analysis to material science. The first one is on a yarn composite SiC where we want to know the relative proportion of matrix, fibers, porosity and the size of the fibers. The results are used to estimate mechanical properties of the composite.

The second one is to measure the residual porosity after a laser shock on powder metallurgy steel. The knowledge of the depth of the affected zone is necessary to optimise the laser treatment.

The third one uses Fourier transformation to analyse plastic deformation on grains. Values are obtained from Fourier transform images.

The last one is to make measurements of the length of cracks on fracture sample, to separate intergranular and transgranular character of a fracture surface.

Key Words : Image analyis, composite, laser treatment, plastic deformation quantification, fracture quantification.

Introduction

The experimental study of materials tends to produce images revealing structure, phase distribution, etc... This information is often limited to one or two photographs which are reputed to correspond to a general description of the entire sample. However this partial information is rarely objective. Image Analysis allows a more objective characterisation of the whole surface to be obtained with numerical values and a statistical approach.

The Image Analysis System used most often in our laboratory is a Noran TN 8502 connected to :

a) a Camera which can be installed on an automated stage optical microscope,
b) a Philips 501 scanning electron microscope (electrons signals),
c) a Cameca SX 50 electron probe micro analyser (electrons and X signals),
4) a Philips 430 scanning transmission electron microscope (electrons and low level camera).

We have studied four applications of Image Analysis :

Stranded Composite SiC-SiC

This composite is formed with bundles of SiC fibers infiltrated by vapor impregnation of SiC. This material is far from being homogeneous, as shown in Figure 1. Measurements are made in two steps : relative proportion of matrix, fibers and porosity are obtained directly on the whole stranded composite using a min-max enhanced contrast filter and automatic thresholding to the minimas of the histogram. Average results are approximately 6% porosity, 38% fibers, 56% matrix. At higher magnification (Figure 2), the diameter of each fiber is measured after thresholding and separation using ultimate erosion (Beucher). Results are shown in Figure 3, for 500 fibers, the mean diameter is 14 µm with a standard deviation of 3. These results are used to estimate mechanical properties of the composite : Young's modulus of these fibers is known to be 200 GPa and that of the matrix to be 350 GPa. Using the rule of mixtures on matrix and fibers, we found 271 GPa for the yarn SiC. Tensile tests on samples give a value of 292 GPa. If the Young's modulus for fibers was well known, this was not the case for the matrix. Indeed, Arnault (1989) computation,

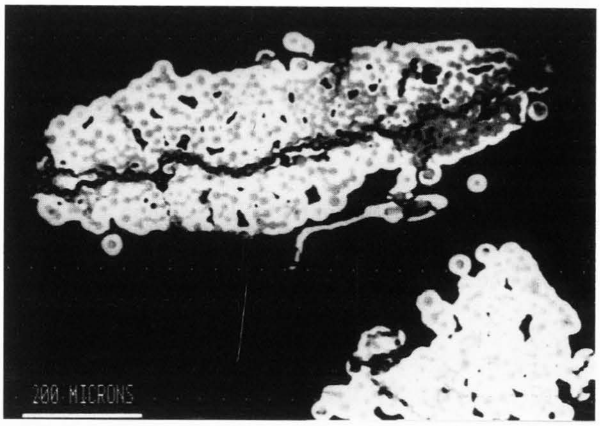

Figure 1. The whole yarn SiC-SiC.

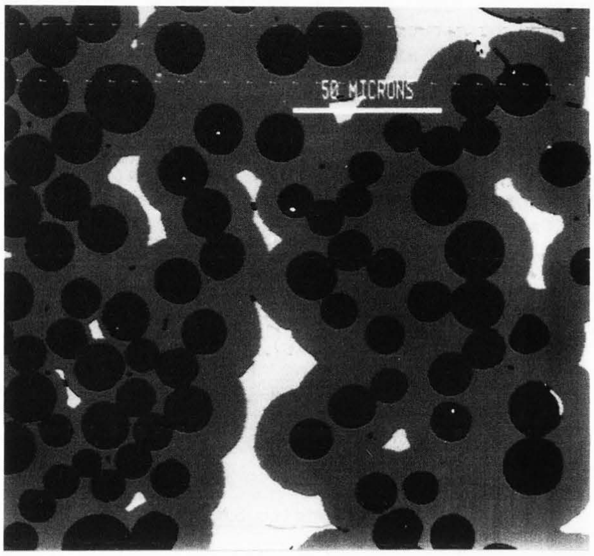

Figure 2. Dipersion in size of SiC fibers.

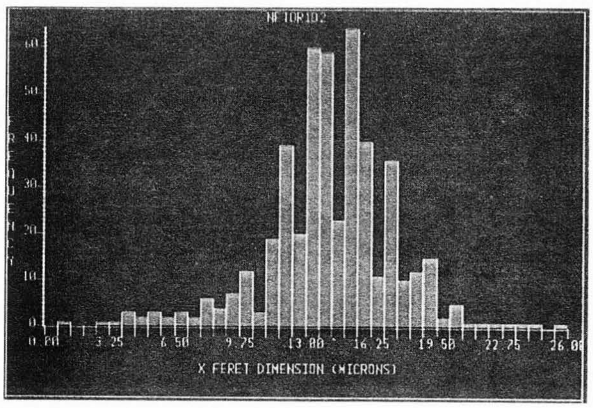

Figure 3. Size distribution of fibers.

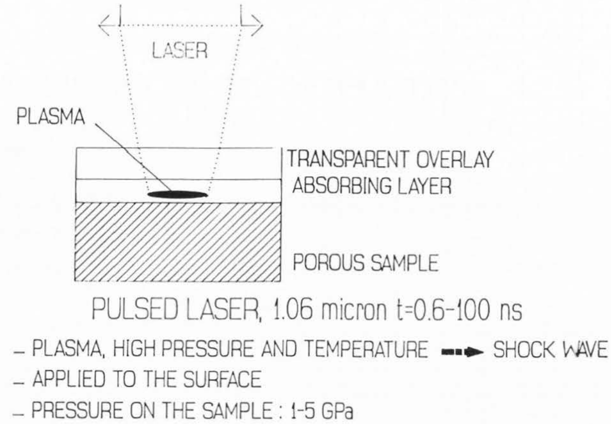

Figure 4. Schematic diagram of pulse laser shock.

using results of X-ray diffraction, has shown that theoretical Young's modulus could be 419 GPa if the crystallographic direction of the matrix is parallel with that of the fibers. So, we can conclude that the manufacturing elaboration process used orientates lightly the matrix deposited on the fibers.

Laser Shock Treated Powder Compacts

Powder metallurgy is increasingly used by industry to obtain low cost components. But this process leaves porosity which can result in lower mechanical properties (especially in fatigue). For friction applications, it may sufficient to eliminate superficial porosity. To do this, tests are made with pulsed laser surface treatments. The sample is, in a first step, painted in black to form a light absorbing layer on the surface. It is then covered with a transparent overlay (piece of glass). When the whole is illuminated by the extremely short and intense laser pulse, a plasma occurs between the surface and the absorbing layer (Figure 4). This plasma induced high pressures and temperatures which provoke a shock wave on the surface with a pressure up to 5 GPa. This process reduces porosity proportionally to the pressure applied (Figure 5), itself controled by the energy and duration of the pulse.

In this case, Image Analysis is used to make measurements of the porosity as a function of depth below the specimen surface. To do this, a binary rectangular mask is moved from the surface, and each time the porosity area inside the mask is measured (Figure 6). We can then correlate the depth of the zone affected by superficial densication and the final residual porosity with the laser pulse generated pressure or initial porosity (Figure 7).

Slip Lines in Nickel Base Superalloys

On samples of nickel base superalloy Inconel 718 with good surface preparation (electrolytic polishing), slip lines develop on the free surface during mechanical test (Figure 8). These lines show the localisation of plastic deformation inside the sample. Fourier transforming on secondary electrons from scanning

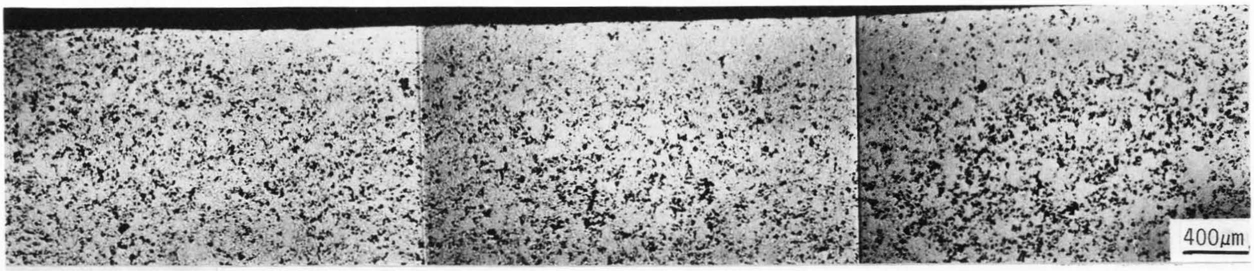

P = 50 kBar t=28ns Por.= 8%

Figure 5. Effect of pressure on porosity. Laser shock on top.

P= 30 kBar t= 28ns Por.= 8%

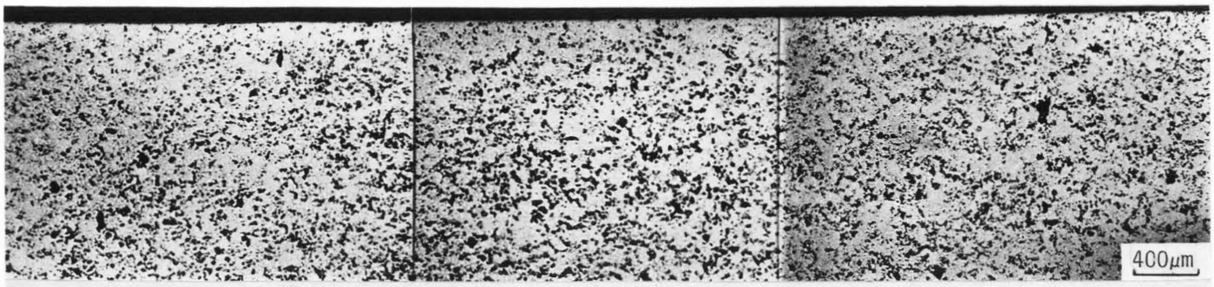

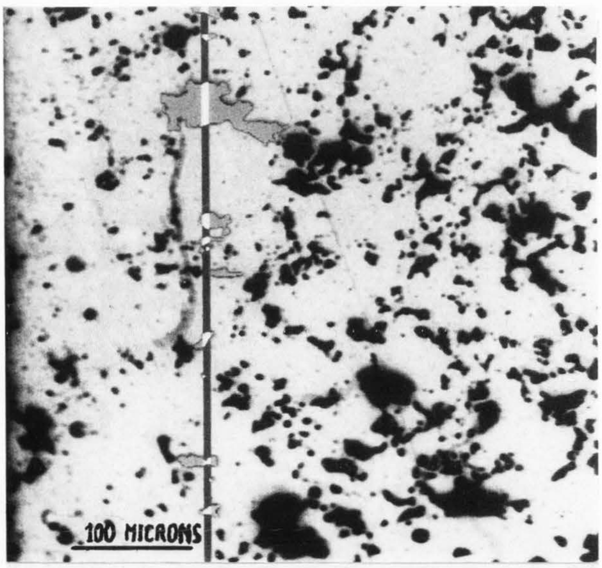

Figure 6. Porosity mask measurement. Laser shock on left side.

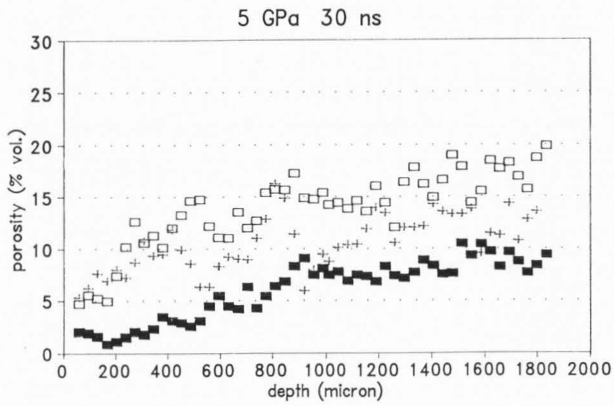

Figure 7. Results curves of porosity.

electron microscopy images of a single grain, extract slip lines (Figure 9). Analysis of this transformation shows the orientation and the frequency of slip lines in regards to the direction of the applied external stresses (Figure 10). Analysis of these slip lines all along the sample should make an image of the stress distribution.

Crack Lengths in Damaged Nickel Base Superalloys

After mechanical test, the fracture surface often shows intergranular and transgranular character. A cut along the sample (nickel base superalloy N 18) shows the irregular roughness of the surface (Figure 11), the right part of figure 11 is transgranular, and the left part is intergranular. The intergranular part shows a longer profile than the transgranular. After extracting the profile, we made an 8 connexity skeleton (Figure 12). Linear length is then measured using three filters in a square grid : horizontal and vertical, diagonal and intermediate with respective weight of 1, $\sqrt{2}$, $\frac{1 + \sqrt{2}}{2}$. This

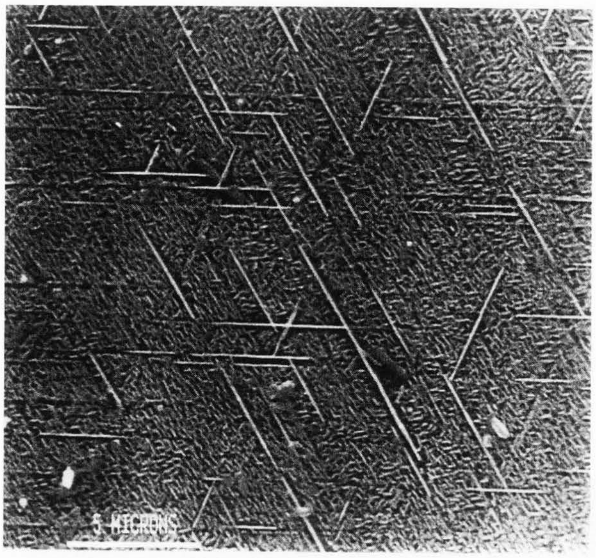

Figure 8. Slip lines developed on Inco 718.

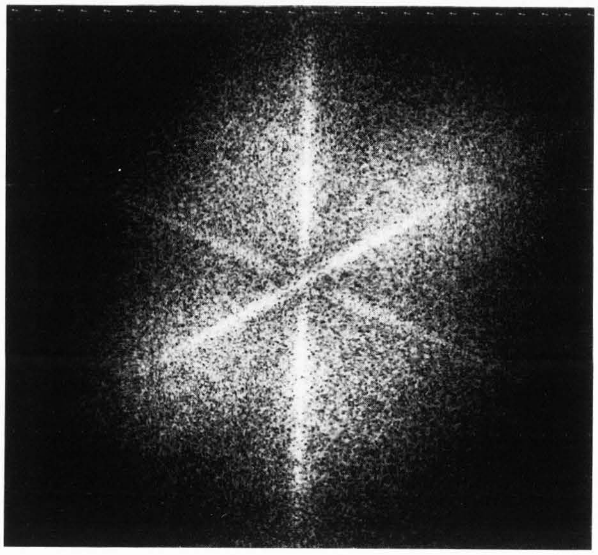

Figure 9. Fourier transform of figure 8.

measure could be in excess of 8% in case of a straightline with a slope of 30° with horizontal. For a more regular form, as a circle, the value of the perimeter is in excess of 5%, due to the digitalisation. In this case the linear length of the transgranular part is 2.5 times the linear length of the interganular part.

This nickel base superalloy is strengthened by precipitates of the gamma prime phase (0.5 µm for the larger fraction). In this study we also tried to determine if this phase delineates a preferential path for crack propagation. Treatment consists of counting this phase along the crack and to compare the result with number of intercepts within a straight line in the matrix. No significant results have been obtained in this case.

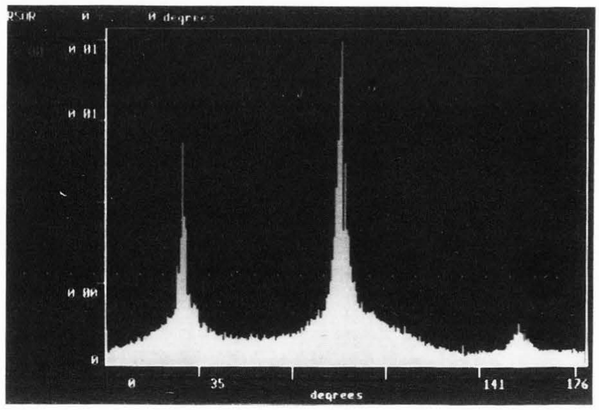

Figure 10. Analyses of orientation and amplitude of slip lines from F.T. image

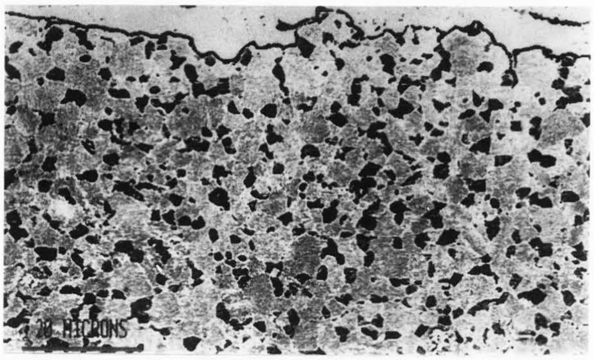

Figure 11. Crack surface of N18 nickel base superalloy.

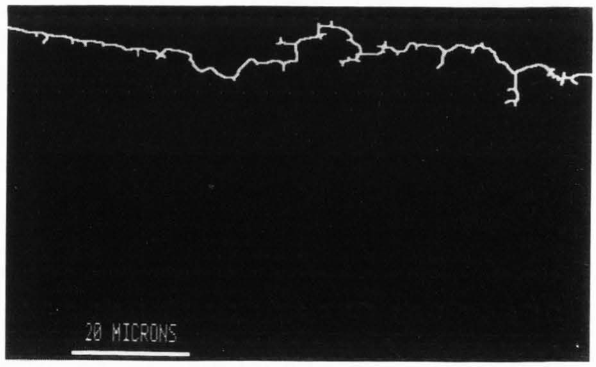

Figure 12. Profile of the crack after skeleton.

Conclusion

Image Analysis in a usefull tool to quantify structure of materials, as shown in these four examples. Many other cases can be solved by this technique. Image Analysis is also a powerfull process for computing model adjustements.

References

ARNAULT, V. (1989), Relations entre microstructure et comportement mécanique des composites SiC/SiC : analyse du rôle de l'interface dans le processus de fissuration matricielle dans des matériaux multifilamentaires (Relation Between microstructure and mechanical behavior of SiC/SiC composites : part of interface in the matrix fissuration process in bundles fibers) pp.120-125. Thèse de Doctorat, Institut National des Sciences Appliquées de Lyon, December 1989.

BEUCHER, S. (1990) Segmentation d'images et morphoplogie mathématique (Image segmentation and mathematical morphology) pp.206-208 Thèse de Doctorat; Ecole Nationale Supérieure des Mines de Paris, 5 June 1990.

Discussion with Reviewers

Reviewer : A powerful tool is described to monitor the effectiness of laser pulses to the porosity of material using electron microscopy and image analysis. Is this image analysis method sufficiently objective to make a comparison between the porosity of different materials possible. Or is the human subjectivity in defining segmentation thresholds a limiting factor?

Author : In this case, high contrasted images are obtained. So, segmentation thresho!d is not a limiting factor. Automatic thresholding can be processing using minimum value of the grey level histrogram of the image making a comparison between different materials possible. The true problem, in this case, is sample preparation which can enlarge porosity. This problem is limiting by a good impregnation process before polishing.